

Consistent Multiple Graph Embedding for Multi-View Clustering

Yiming Wang, Dongxia Chang, Zhiqiang Fu and Yao Zhao, *Senior Member, IEEE*

Abstract—Graph-based multi-view clustering aiming to obtain a partition of data across multiple views, has received considerable attention in recent years. Although great efforts have been made for graph-based multi-view clustering, it remains a challenge to fuse characteristics from various views to learn a common representation for clustering. In this paper, we propose a novel Consistent Multiple Graph Embedding Clustering framework(CMGE). Specifically, a multiple graph auto-encoder(M-GAE) is designed to flexibly encode the complementary information of multi-view data using a multi-graph attention fusion encoder. To guide the learned common representation maintaining the similarity of the neighboring characteristics in each view, a Multi-view Mutual Information Maximization module(MMIM) is introduced. Furthermore, a graph fusion network(GFN) is devised to explore the relationship among graphs from different views and provide a common consensus graph needed in M-GAE. By jointly training these models, the common latent representation can be obtained which encodes more complementary information from multiple views and depicts data more comprehensively. Experiments on three types of multi-view datasets demonstrate CMGE outperforms the state-of-the-art clustering methods.

Index Terms—Multi-view Clustering, Graph Neural Networks, Representation Learning, Mutual Information.

I. INTRODUCTION

WITH the advance of information technology, multiple views of objects can be readily acquired in many domains. For instance, a piece of news can be reported by multiple news organizations, and an image can be described in different features: GIST [1], SIFT [2], LBP [3], and HOG [4], *etc.* Compared with single-view data, these multi-view data provide more comprehensive characteristics and useful information [5], [6]. With the emergence of multi-view data, multi-view clustering method arises at the historic moment, and it can boost clustering performance by integrating different views. However, there are a number of challenges to multi-view clustering. Large differences in data from different views may produce view disagreement which can distort a similarity matrix used to depict samples within the same class [7], [8]. Additionally, the dimension difference of features from different views can lead to difficulties in feature fusion [9].

To solve the above problems, numerous multi-view clustering methods have been proposed. Among them, graph-based multi-view clustering method [10], [11], [12] is one kind of the more widely used algorithms. These methods seek to find

Y. Wang, D. Chang, Z. Fu and Y. Zhao are with the Institute of Information Science, Beijing Jiaotong University, Beijing 100044, China, and also with Beijing Key Laboratory of Advanced Information Science and Network Technology, Beijing 100044, China (e-mail: wangym@bjtu.edu.cn; dxchang@bjtu.edu.cn zhiqiangfu@bjtu.edu.cn; yzhao@bjtu.edu.cn).

a fusion graph across all views and use graph-cut algorithms or other technologies (e.g., spectral clustering) on the fusion graph to produce the clustering result. The approaches can solve the problem that dimensional differences of different views to some degree. However, these graph-based multi-view clustering methods are generally shallow models, which have limited capacity to reveal the relations in complex multi-view data. Moreover, these shallow models can hardly combine graph structural information with data intrinsic characteristics. However, structural information and node characteristics are equally important for clustering tasks.

The Graph Convolutional Networks(GCN) [13], [14] recently emerged can encode both of the graph structure and the node characteristics for node latent representation. And many GCN-based clustering methods [15], [16] have been proposed. AGAE [17] employs graph representation learning techniques to ensemble clustering task to jointly integrate the information from node content and consensus graph. To achieve mutual benefit for both learned embedding and graph clustering, DAEGC [15] proposes a goal-directed graph attentional autoencoder based attributed graph clustering framework. The above methods typically learn a graph embedding from a predefined graph and feature matrix. And the clustering results are obtained by conventional clustering methods. These GCN based methods greatly improve the performance of graph-based clustering. However, all these methods can handle single view data and there are few GCN-based multi-view clustering algorithms. To model multi-view graph information, O2MAC [18] proposes a one-to-multi graph autoencoder for multi-graph clustering, which employing one informative graph view to reconstruct multiple graph views to capture the shared representation of multiple graphs. Unlike the general multi-view clustering method applied to multi-view data and graph, it is employed for single-view data with multi-view graph. These methods apply GCN to exploits both graph structure and nodes content to learn a latent representation. However, the graph in most GCN-based methods is fixed, which makes the clustering performance heavily dependent on the predefined graph. And a noisy graph with unreliable connections can result in ineffective convolution with wrong neighbors on the graph [19], which may worsen performance.

In order to solve the above challenges in multi-view clustering, we propose a Consistent Multiple Graph Embedding Clustering framework(CMGE), which is mainly composed of Multiple Graph Auto-Encoder(M-GAE), Multi-view Mutual Information Maximization module(MMIM) and Graph Fusion Network(GFN). Our major contributions can be summarized as follows:

- In order to well capture the complementary information and internal relations of each view, we propose a multi-graph attention fusion encoder to adaptively learn a common representation from multiple views.
- To maintain consistency within views, multi-view mutual information maximization is devised to make similar instances still similar to each other in the common space.
- To explore the relationships among different view graphs, a graph fusion network is devised to fuse graphs from multiple views to get a consensus graph needed in the multiple graph auto-encoder. And to improve the separability of the consensus graph, the rank constraint on its Laplacian matrix is utilized to train the GFN.
- We have conducted experiments on three types of multi-view data, including multi-view data without graph, multi-view data with common graph and single-view data with multi-graph. And experiments on these datasets show that our CMGEC outperforms state-of-the-art clustering methods.

II. RELATED WORKS

Before introducing the proposed CMGEC, graph-based multi-view clustering and mutual information maximization are briefly introduced in this section.

a) Graph-based multi-view clustering: For the graph-based multi-view clustering methods, the view-specific graphs are constructed based on the k -NN graph and used to find a fusion graph across all views. Finally, the clustering assignment is obtained based on the fusion graph. Most graph-based multi-view clustering methods are based on the spectral clustering, which is a classic data clustering algorithm aiming to build a normalized affinity matrix and compute the eigenvectors of this normalized affinity matrix. Combined with graph fusion, it can be extended to multi-view clustering. Based on spectral partitioning and local refinement, Chikhi [20] presents a parameter free multi-view spectral clustering algorithm. To address the issue that dependencies among views often delude correct predictions, Son et al. [21] propose a spectral clustering method to deal with multi-view data and dependencies among views based on the brainstorming process. In order to solve the problem that graph-based clustering highly depends on the quality of a predefined graph, MVGL [22] learns a global graph, which has an exact number of the connected components that reflects cluster indicators. To further improve the performance and simplify the model, Zhan et al. [23] leverages the common consensus information derived from the connections between diverse views and proposes an overall objective function. To sufficient consider weights of different views, GMC [24] couples the learning of the similarity-induced graphs, the unified graph, and the clustering task into a joint clustering framework. However, one major drawback of these shallow models is that they have limited capacity to reveal the deep relations in complex graph data.

b) Mutual information maximization: To maintain the consistency of similar samples in each view, we employ mutual information maximization in our model. Mutual information is a Shannon entropy-based fundamental quantity

for measuring the relationship between random variables [25]. Following the works in RIM [26], maximizing the mutual information between input samples and latent cluster assignments can be used in discriminative clustering. And this concept is further studied by some deep clustering methods [25], [27], which learns discriminative neural network classifiers that maximize the mutual information. Generally, the problem corresponds to maximizing the following objective:

$$I(X, K) = H(K) - H(K|X) \quad (1)$$

where $H(\cdot)$ and $H(\cdot|\cdot)$ are the entropy and conditional entropy, respectively. $K \in \{1, \dots, \mathbb{K}\}$ and $X \in \mathbb{X}$ denote random variables for cluster assignments and data samples, respectively. And the mutual information between sample X and latent representation Z can be understood as:

$$\begin{aligned} I(X, Z) &= \iint p(z|x)p(x) \log \frac{p(z|x)}{p(z)} dx dz \\ &= KL(p(z|x)p(x) || p(z)p(x)) \end{aligned} \quad (2)$$

where $p(x)$ is the distribution of the input samples and $p(z|x)$ is the distribution of the latent representations. The distribution of the latent space $p(z)$ can be calculated by $p(z) = \int p(z|x)p(x)dx$. And adversarial learning can be used to constrain the latent representations to have desired statistical characteristics specific to the input samples.

III. THE PROPOSED MODEL

As aforementioned, current graph-based multi-view clustering methods have the following shortcomings: (1) the shallow model can hardly combine the graph structural information with the node intrinsic characteristics; (2) the GCN-based methods generally use fixed graph structure, thus its performance depends heavily on the predefined graph. To handle these two challenges, CMGEC is proposed and the overall framework is shown in Fig. 1. Our CMGEC mainly contains three parts: M-GAE, MMIM and GFN. Firstly, the predefined graph of each view is input into the GFN to obtain the consensus graph. In order to make the consensus graph more sparse and cluster-friendly, the rank constraint on its Laplacian matrix is used to train the GFN. Then the raw features, the graph of each view and the consensus graph are fed into the M-GAE to learn a common latent representation. To flexibly incorporate information from all views, multi-graph attention fusion encoder is introduced into the M-GAE. Moreover, MMIM is devised to make the learned common representation maintain the similarity of the neighboring characteristics. In the following, we will describe our proposed model in detail.

Formally, given a multi-view dataset $\mathcal{X} = \{X^{(1)}, \dots, X^{(v)}\}$ consisting of n samples from v views, $X^{(v)} \in \mathbb{R}^{d_v \times n}$ denotes the feature matrix in the v -th view. And d_v is the dimension of v -th view samples. $\mathcal{A} = \{A^{(1)}, \dots, A^{(v)}\} \in \mathbb{R}^{n \times n}$ represents the graph of each view. A^* denotes the common graph where $A^* = f(\mathcal{A}; \theta_g) \in \mathbb{R}^{n \times n}$ is learned by the GFN. The parameters of the GFN are defined by θ_g . Z denotes the common latent representation where $Z = f(\mathcal{X}, \mathcal{A}, A^*; \theta_e) \in \mathbb{R}^{m \times m}$ is learned by the multiple graph fusion encoder E . The parameters of the encoder are defined by θ_e , and

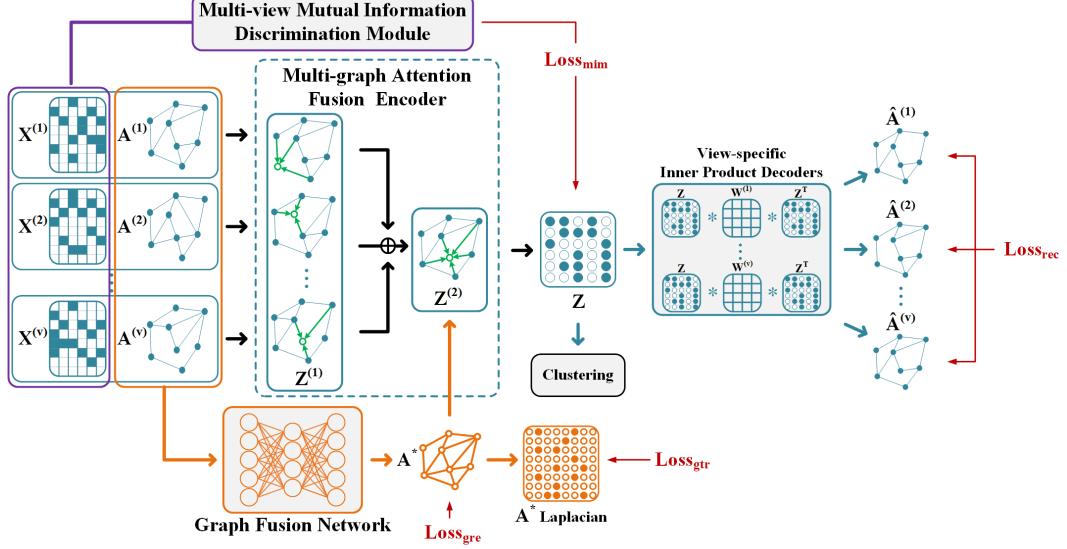


Fig. 1. The framework of the proposed CMGEC. It consists of three main components: Multiple Graph Auto-Encoder(M-GAE), Multi-view Mutual Information Maximization module(MMIM), and Graph Fusion Network(GFN).

m is the dimension of the learned common representation. $\hat{A}^{(1)}, \dots, \hat{A}^{(v)} = f(z; \theta_d) \in \mathbb{R}^{m \times m}$ represent the reconstructed graph data, which are the output of the view-specific decoders D , and the parameters of the decoder are denoted by θ_d .

A. Multiple Graph Auto-Encoder

In order to represent both multi-view graph structure \mathcal{A} and nodes feature \mathcal{X} comprehensively in a unified framework, we develop a M-GAE in which common latent representation are learned by a multi-graph attention fusion encoder. Moreover, the view-specific decoders are designed to reconstruct multi-view graph data from the learned representation.

a) *Multi-Graph Attention Fusion Encoder*: To learn a common representation that can fully integrate information from multiple views, a multi-graph attention fusion layer, which can fuse multi-view data and graphs adaptively, is devised based on the GCN [13]. After getting the common representation, the final representation Z can be obtained by the GCN using the common representation and graph. Here, the common graph is obtained by GFN and we will introduce it in detail in next section.

The GCN extends the operation of convolution to graph data in the spectral domain. Here, $Z_{(l)}$ is the representation learned by the l -th layer of GCN and it can be obtained by the following graph convolutional operation:

$$Z_{(l)} = \phi \left(\tilde{D}^{-\frac{1}{2}} \tilde{A} \tilde{D}^{-\frac{1}{2}} Z_{(l-1)} W_{(l)} \right) \quad (3)$$

where $\tilde{A} = A + I$ and $\tilde{D}_{ii} = \sum_j \tilde{A}_{ij}$. I is the identity diagonal matrix, $W_{(l)}$ denotes the learned parameter matrix, and $\phi(\cdot)$ is an activation function.

In the multi-graph attention fusion encoder, the first layer is composed of v view-specific GCN layers, and the input of the first layer are multi-view data $\mathcal{X} = \{X^{(1)}, \dots, X^{(v)}\}$ and the corresponding graphs $\mathcal{A} = \{A^{(1)}, \dots, A^{(v)}\}$. Then, the v -

th view-specific representations $Z_{(1)}^{(v)}$ learned by the first layer can be obtained by:

$$Z_{(1)}^{(v)} = \phi \left((\tilde{D}^{(v)})^{-\frac{1}{2}} \tilde{A}^{(v)} (\tilde{D}^{(v)})^{-\frac{1}{2}} X^{(v)} W_{(1)}^{(v)} \right) \quad (4)$$

In order to flexibly integrate the view-specific representation, a multi-graph attention fusion layer is devised using attention strategy. Different from graph attention network [28] that learn hidden representations of each node by weighting the representations for each nearest neighbor in the same view, our approach focuses on the weighting of different views. To adaptively fuse the representation of a sample in different views, attention coefficient matrix W_a is introduced to learn the importance of different views. Hence, the common representation learned by the multi-graph attention fusion layer can be obtained by the following operation:

$$Z_{(2)} = \phi \left(\sum_{v=1}^V W_a \left((\tilde{D}^{(v)})^{-\frac{1}{2}} \tilde{A}^{(v)} (\tilde{D}^{(v)})^{-\frac{1}{2}} Z_{(1)}^{(v)} W_{(2)}^{(v)} \right) \right) \quad (5)$$

Then a GCN layer is used to provide the final common representation Z :

$$Z = \phi \left((\tilde{D}^*)^{-\frac{1}{2}} \tilde{A}^* (\tilde{D}^*)^{-\frac{1}{2}} Z_{(2)} W_{(3)} \right) \quad (6)$$

where A^* is the consensus graph learned by GFN, and $\tilde{D}_{ii}^* = \sum_j \tilde{A}_{ij}^*$.

b) *View-specific Graph Decoders*: In order to supervise the multi-graph fusion encoder to learn a comprehensive common representation, view-specific graph decoders are applied to reconstruct the multi-view graph data $\hat{A}^{(1)}, \dots, \hat{A}^{(v)}$ from the learned representation Z . As the learned representation already contains both contents and structure information, inner product decoders are adopted to predict the links between nodes, which can be written as:

$$\hat{A}^{(v)} = \text{sigmoid}(Z \cdot W^{(v)} \cdot Z^T) \quad (7)$$

where $W^{(v)}$ is the learned parameter matrix in the v -th view-specific decoder.

c) *Reconstruction loss*: To train the M-GAE, we minimize the sum of reconstruction error of each view by measuring the difference between $A^{(v)}$ and $\hat{A}^{(v)}$:

$$L_{rec} = \sum_{v=1}^V L_{rec}^{(v)} = \sum_{v=1}^V loss(A^{(v)}, \hat{A}^{(v)}) \quad (8)$$

where $L_{rec}^{(v)}$ is the reconstruction loss for view v and L_{rec} is the reconstruction loss for all views.

B. Graph Fusion Network

Multi-view data and graphs provide multiple independent and complementary information from multiple feature spaces, and their analysis can often result in more integrated and accurate results than single view [29]. However, each graph contains different adjacency relations in different views and cannot be used directly in the common space. Therefore, to explore relationships among different views and provide global nodes relationship, a graph fusion network is devised to produce consensus graph A^* .

In our model, a fully connected network is employed to learn the consensus graph. Specifically, the consensus graph learned by the l -th layer in the graph fusion network can be described as:

$$G_{(l)} = \phi(W_{g(l)}G_{(l-1)} + b_{g(l)}) \quad (9)$$

where ϕ is the activation function of the fully connected layers, $W_{g(l)}$ and $b_{g(l)}$ are the weight matrix and bias of the l -th layer in the graph fusion network, respectively. To adaptively fuse each graph, a multi-graph fusion layer is placed on the first layer of GFN, and it is defined as:

$$G_{(1)} = \phi\left(\sum_{v=1}^V W_f(W_{g(1)}^{(v)} A^{(v)} + b_{g(1)}^{(v)})\right) \quad (10)$$

where W_f is the attention coefficient matrix that indicates the importance of the edge in different views.

In order to combine the features of each graph and make the consensus graph A^* more suitable for clustering, the loss of the graph fusion network is defined as

$$\begin{aligned} L_G &= L_{gre} + \lambda_1 L_{gtr} \\ &= \sum_{v=1}^V loss(A^{(v)}, A^*) + \text{tr}(Q^T L_{A^*} Q) \\ &\text{s.t. } Q^T Q = I \end{aligned} \quad (11)$$

where L_{gre} and L_{gtr} are the graph reconstruction loss for all views and the Ratio Cut used spectral clustering, respectively. $\text{tr}(\cdot)$ is the trace operator. L_{A^*} is the Laplacian matrix of A^* and Q is the relaxed indicator which can be computed by the eigenvalue decomposition of L_{A^*} . λ_1 is a hyperparameter that balances these two losses.

Obviously, the consensus graph A^* can be segmented directly to obtain the clustering results. Since the GFN uses only the graph structure and ignores the intrinsic characteristics of nodes, the clustering result obtained using A^* is worse than that of the learned common representation.

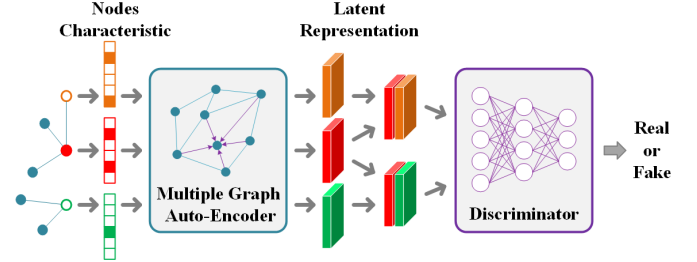


Fig. 2. The architecture of MMIM. In the training process, we select k_M nearest neighbors for each nodes in each view. And the positive pairs are composed of the common representation of nodes and their nearest neighbors. Meanwhile, the same number of nodes besides the nearest neighbors are randomly selected. And the negative pairs consist of the common representation of nodes and these random nodes. Finally, a discriminator is used to distinguish these pairs.

C. Multi-view Mutual Information Maximization

In the fields of subspace learning, a recognized assume is that if two samples are close to each other, their corresponding low dimensional representations should also be close in the latent space [30]. Therefore, the inter-sample information can be used to guide the autoencoder to learn more cluster-friendly representation.

In our model, we assume that if two samples x and x' are close in any view, then their corresponding representations z and z' should also be close in the common view. Based on the assumption, a multi-view mutual information maximization module(MMIM) is devised to boost the similarity of inter-neighbour representations. And the mutual information maximization module is shown in Fig. 2.

Since larger mutual information denotes the representations are more similar, the mutual information is expected to be as large as possible and the objective of MMIM can be described as

$$\max\{I(X, Z')\} \quad (12)$$

According Eq.(2) and Eq.(12), the loss function of MMIM L_{mim} can be written as

$$L_{mim} = -KL(p(z'|x)p(x)||p(z')p(x)) \quad (13)$$

However, KL divergence is unbounded. Therefore, we use JS divergence instead of KL divergence in mutual information and Eq.(13) can be converted to

$$L_{mim} = -JS(p(z'|x)p(x)||p(z')p(x)) \quad (14)$$

According to [31], the variational estimation of JS divergence between two distributions $p(x)$ and $q(x)$ is defined as

$$\begin{aligned} JS(p(x)||q(x)) &= \mathbb{E}_{x \sim p(x)}[\log p(T(x))] \\ &+ \mathbb{E}_{x \sim q(x)}[\log(1 - p(T(x)))] \end{aligned} \quad (15)$$

where $T(x) = \log \frac{2p(x)}{p(x)+q(x)}$ [31]. In our loss function, $p(z'|x)p(x)$ and $p(z')p(x)$ are used to replace $p(x)$ and $q(x)$. Hence, substituting Eq.(15) into Eq.(14) yields

$$\begin{aligned} L_{mim} &= -\mathbb{E}_{(x, z') \sim p(z'|x)p(x)}[\log p(T(x, z'))] \\ &- \mathbb{E}_{(x, z') \sim p(z')p(x)}[\log(1 - p(T(x, z')))] \end{aligned} \quad (16)$$

TABLE I
DATASETS STATISTICS OF MULTI-VIEW DATA WITHOUT PREDEFINED ATTRIBUTE GRAPH.

Datasets	Classes	Nodes	Feature1	Feature2	Feature3	Feature4
3source	6	169	3560	3631	3068	-
BBC	5	685	4659	4633	4665	4684
100LEAVES	100	1600	64	64	64	-
Cub	200	6033	1024	300	-	-

TABLE II
DATASETS STATISTICS OF MULTI-VIEW DATA WITH COMMON ATTRIBUTE GRAPH.

Datasets	Classes	Nodes	Edges	Attribute1	Attribute2
Cora	7	2708	5429	1433	2708
Citeseer	6	3327	4732	3703	3327
Pubmed	3	19717	44438	19717	500

Here, negative sample estimation [27] is used to solve the problem in Eq.(16). Positive and negative sample pairs are generated by the latent representations. Then a discriminator is used to distinguish the negative sample pairs and positive sample pairs to estimate the distribution of positive samples. In Eq.(16), $\rho(T(x, z'))$ is a discriminator, and the representation of sample x and its nearest neighbors x' compose positive pairs. And the negative pairs are composed of the representation of x and random representations outside the nearest neighbors. For each samples, k_M nearest neighbors are selected to compose positive pairs in all views. For data without graph, we use k -NN algorithm to find the nearest neighbors. And for data with attributed graph, we use a modified Shared Nearest Neighbor(SNN) [32] similarity to find the nearest neighbors on the attributed graph. The modified SNN similarity can be written as

$$sim(i, j) = \begin{cases} 0, & \text{No edge between } v_i \text{ and } v_j, \\ |\mathcal{N}(i) \cap \mathcal{N}(j)|, & v_i \text{ and } v_j \text{ are adjacent.} \end{cases} \quad (17)$$

where $\mathcal{N}(*)$ denotes the neighboring nodes of v_* . After getting the similarity of all other points to v_* , the k_M most similar nodes are selected as the nearest neighbors of v_* .

Thus the total objective function of M-GAE module is defined as:

$$L_M = L_{rec} + \lambda_2 L_{mim} \quad (18)$$

where λ_2 is a hyperparameter that balances these two loss functions.

IV. EXPERIMENTS

In this section, we evaluate the performance of the proposed CMGEC for multi-view clustering on three types popular real-world databases, including multi-view data without graph, multi-view data with common graph and single-view data with multi-graph.

A. Experimental Settings

a) *Datasets:* In order to fully evaluate the effectiveness of the proposed algorithm, we conduct experiments on the

TABLE III
DATASETS STATISTICS OF SINGLE-VIEW DATA WITH MULTIPLY ATTRIBUTE GRAPHS.

Datasets	Classes	Nodes	Dimension	Edge1	Edge2	Edge3
DBLP	4	4057	334	11113	5000495	6776335
IMDB	3	4780	1232	98010	21018	-
ACM	3	3025	1830	29281	2210761	-

following three types of multi-view data. For convenience, these datasets are summarized in Table I, II and III.

Multi-view data without predefined attribute graph. *3Source*¹ consists of 169 news, which were reported by three news organizations. And each news was manually annotated with one of 6 topical labels. *BBC*² is a collection of 685 documents associated with 4 views taken from articles in 5 topical areas. *100Leaves*³ consists of 1,600 samples from each of 100 plant species. For each sample, shape descriptor, fine scale margin and texture histogram are given. *Cub*⁴ [40] is an image dataset with photos of 200 bird species. The deep visual features from GoogLeNet [41] and text features from doc2vec [42] are used as two views.

Multi-view data with common attribute graph. We conduct experiments on three widely-used citation network datasets including Cora, Citeseer and Pubmed⁵. The general graph dataset contains one graph and one attribute and there is no graph dataset with multi-view attributes at present. In order to evaluate the method, we use Cartesian product to construct additional attribute view by original attributes.

Single-view data with multiply attribute graphs. We follow the setting used in [18] to build three datasets. *DBLP*⁶ is an author network from the DBLP dataset. We exploit three relationships including the co-authorship, co-conference, and co-term to construct three view graphs. And to evaluate the method, authors' research area are used as ground truth. *IMDB*⁷ is a movie network from the IMDB dataset. Co-actor relationship and co-director relationship are applied to construct two view graphs. And the movies' genre are used as ground truth. *ACM*⁸ is a paper network from the ACM dataset. Two view graphs are constructed from co-paper and co-subject respectively. And papers' research area are used as ground truth.

b) *Evaluation Metrics:* For a comprehensive investigation, we evaluate the performance using five statistical metrics: Accuracy (ACC), Normalized Mutual Information (NMI), Adjusted Mutual Information (AMI), Adjusted Rand Index (ARI) and F1 measure(F1). Generally, the higher values of these five measures mean the better clustering quality. And we perform all algorithm 10 times and report the average results with the standard deviation.

¹<http://mlg.ucd.ie/datasets/3sources.html>

²<http://mlg.ucd.ie/datasets/segment.html>

³<https://archive.ics.uci.edu/ml/datasets/One-hundred+plant+species+leaves+data+set>

⁴<http://www.vision.caltech.edu/visipedia/CUB-200.html>

⁵<https://linqs.soe.ucsc.edu/data>

⁶<https://dblp.uni-trier.de/>

⁷<https://www.imdb.com/>

⁸<http://dl.acm.org>

TABLE IV
PERFORMANCE COMPARISONS OF DIFFERENT METHODS ON MULTI-VIEW DATA WITHOUT PREDEFINED ATTRIBUTE GRAPH.

Datasets	Methods	ACC	NMI	ARI	AMI	F1
3Sources	KM [33]	0.5390 \pm 0.0647	0.4320 \pm 0.1035	0.2880 \pm 0.1300	0.4000 \pm 0.1094	0.3260 \pm 0.0815
	GAE [34]	0.6765 \pm 0.0155	0.5756 \pm 0.0476	0.4553 \pm 0.0446	0.5535 \pm 0.0499	0.6317 \pm 0.0136
	DAEGA [35]	0.7160\pm0.0000	0.6066 \pm 0.0000	0.6208\pm0.0000	0.6135\pm0.0000	0.6470\pm0.0000
	SDCN [36]	0.6252 \pm 0.0028	0.4230 \pm 0.0088	0.4225 \pm 0.0143	0.3921 \pm 0.0096	0.3487 \pm 0.0032
	PMSC [37]	0.4479 \pm 0.0939	0.1461 \pm 0.0583	0.1353 \pm 0.0959	0.1672 \pm 0.0540	0.4310 \pm 0.0394
	MCGC [23]	0.5444 \pm 0.0000	0.4254 \pm 0.0000	0.4270 \pm 0.0000	0.4573 \pm 0.0000	0.5650 \pm 0.0000
	MVGL [22]	0.4550 \pm 0.0000	0.4810 \pm 0.0000	0.4072 \pm 0.0000	0.4755 \pm 0.0000	0.4586 \pm 0.0000
	GMC [24]	0.6923 \pm 0.0000	0.6216\pm0.0000	0.4431 \pm 0.0000	0.6044 \pm 0.0000	0.6047 \pm 0.0000
	AE ² -NET [38]	0.4929 \pm 0.0198	0.3884 \pm 0.0126	0.3268 \pm 0.0151	0.3399 \pm 0.0131	0.4348 \pm 0.0143
	RMSL [39]	0.5219 \pm 0.0671	0.4840 \pm 0.0567	0.3912 \pm 0.0199	0.4560 \pm 0.0603	0.4851 \pm 0.0454
	CMGEC	0.7653\pm0.0307	0.6694\pm0.0143	0.6049\pm0.0446	0.6515\pm0.0147	0.6634\pm0.0355
BBC	KM [33]	0.5201 \pm 0.0673	0.3516 \pm 0.0732	0.2180 \pm 0.1006	0.3458 \pm 0.0745	0.4147 \pm 0.0764
	GAE [34]	0.6397 \pm 0.0066	0.5265 \pm 0.0291	0.4720 \pm 0.0437	0.5228 \pm 0.0292	0.6260 \pm 0.0142
	DAEGA [35]	0.6746 \pm 0.0000	0.5278 \pm 0.0000	0.4661 \pm 0.0000	0.5121 \pm 0.0000	0.6606 \pm 0.0001
	SDCN [36]	0.7156 \pm 0.0044	0.5713 \pm 0.0020	0.5082 \pm 0.0067	0.5664 \pm 0.0020	0.4775 \pm 0.0020
	PMSC [37]	0.6349 \pm 0.0014	0.3124 \pm 0.0020	0.3573 \pm 0.0014	0.3289 \pm 0.0082	0.3822 \pm 0.0007
	MCGC [23]	0.6606 \pm 0.0000	0.3547 \pm 0.0000	0.3085 \pm 0.0000	0.4046 \pm 0.0000	0.3759 \pm 0.0000
	MVGL [22]	0.6620 \pm 0.0000	0.3475 \pm 0.0000	0.3001 \pm 0.0000	0.3934 \pm 0.0000	0.3721 \pm 0.0000
	GMC [24]	0.6891 \pm 0.0000	0.5577 \pm 0.0000	0.4745 \pm 0.0000	0.5611 \pm 0.0000	0.6306 \pm 0.0000
	AE ² -NET [38]	0.7120 \pm 0.0136	0.4192 \pm 0.0044	0.4125 \pm 0.0038	0.4103 \pm 0.0041	0.6200 \pm 0.0197
	RMSL [39]	0.8365\pm0.0303	0.6438\pm0.0350	0.6816\pm0.0350	0.6410\pm0.0353	0.7239\pm0.0493
	CMGEC	0.8737\pm0.0061	0.7144\pm0.0119	0.7392\pm0.0115	0.7121\pm0.0120	0.8623\pm0.0069
100Leaves	KM [33]	0.6134 \pm 0.0087	0.8120 \pm 0.0038	0.4914 \pm 0.0108	0.6841 \pm 0.0065	0.5940 \pm 0.0091
	GAE [34]	0.2875 \pm 0.0180	0.6545 \pm 0.0110	0.1772 \pm 0.0124	0.4525 \pm 0.0128	0.2664 \pm 0.0224
	DAEGA [35]	0.5625 \pm 0.0000	0.7988 \pm 0.0003	0.3850 \pm 0.0004	0.7869 \pm 0.0002	0.5161 \pm 0.0006
	SDCN [36]	0.3683 \pm 0.0465	0.6737 \pm 0.0301	0.2406 \pm 0.0424	0.4626 \pm 0.0489	0.3451 \pm 0.0485
	PMSC [37]	0.5459 \pm 0.0165	0.4292 \pm 0.0253	0.4927 \pm 0.0159	0.4369 \pm 0.0164	0.3081 \pm 0.0153
	MCGC [23]	0.7694 \pm 0.0000	0.8544 \pm 0.0000	0.4924 \pm 0.0000	0.7926 \pm 0.0000	0.4987 \pm 0.0000
	MVGL [22]	0.8106 \pm 0.0000	0.8912 \pm 0.0000	0.5155 \pm 0.0000	0.8557\pm0.0000	0.5217 \pm 0.0000
	GMC [24]	0.8238\pm0.0000	0.9292\pm0.0000	0.4974 \pm 0.0000	0.8479 \pm 0.0000	0.5042 \pm 0.0000
	AE ² -NET [38]	0.7500 \pm 0.0210	0.8880 \pm 0.0134	0.6714\pm0.0316	0.8106 \pm 0.0224	0.7288\pm0.0226
	RMSL [39]	0.6483 \pm 0.0049	0.8047 \pm 0.0096	0.4904 \pm 0.0014	0.6683 \pm 0.0158	0.5176 \pm 0.0160
	CMGEC	0.9156\pm0.0070	0.9684\pm0.0025	0.8876\pm0.0067	0.9461\pm0.0042	0.9086\pm0.0077
Cub	KM [33]	0.7243 \pm 0.0129	0.7085 \pm 0.0032	0.5543 \pm 0.0083	0.6992 \pm 0.0033	0.7325 \pm 0.0129
	GAE [34]	0.7917 \pm 0.0325	0.7904 \pm 0.0138	0.6936 \pm 0.0238	0.7837 \pm 0.0143	0.7843 \pm 0.0343
	DAEGA [35]	0.7467 \pm 0.0005	0.7328 \pm 0.0001	0.6125 \pm 0.0000	0.7337 \pm 0.0003	0.7345 \pm 0.0002
	SDCN [36]	0.8025\pm0.0415	0.7894 \pm 0.0211	0.7045\pm0.0199	0.7749 \pm 0.0201	0.7851\pm0.0254
	PMSC [37]	0.7179 \pm 0.0014	0.7548 \pm 0.0031	0.6397 \pm 0.0009	0.7501 \pm 0.0026	0.6673 \pm 0.0006
	MCGC [23]	0.7454 \pm 0.0000	0.7959\pm0.0000	0.6499 \pm 0.0000	0.7842 \pm 0.0000	0.6790 \pm 0.0000
	MVGL [22]	0.7491 \pm 0.0000	0.7972\pm0.0000	0.6571 \pm 0.0000	0.7891\pm0.0000	0.6853 \pm 0.0000
	GMC [24]	0.7333 \pm 0.0000	0.7947 \pm 0.0000	0.6467 \pm 0.0000	0.7884 \pm 0.0000	0.6862 \pm 0.0000
	AE ² -NET [38]	0.7677 \pm 0.0292	0.7666 \pm 0.0255	0.6458 \pm 0.0445	0.7589 \pm 0.0264	0.7518 \pm 0.0177
	RMSL [39]	0.7423 \pm 0.0096	0.7231 \pm 0.0192	0.6072 \pm 0.0194	0.7142 \pm 0.0198	0.6484 \pm 0.0177
	CMGEC	0.8467\pm0.0041	0.7951 \pm 0.0059	0.7117\pm0.0064	0.7980\pm0.0061	0.8465\pm0.0043

c) *Comparison Algorithms*: We compare the proposed CMGEC with some single-view clustering methods and several state-of-the-art multi-view clustering as baselines.

Single-view clustering methods: K-means++(KM) [33], graph autoencoder(GAE) [34], deep attentional embedding graph clustering(DAEGA) [35], and structural deep clustering network(SDCN) [36]. For the single view clustering methods, we report their results of the most informative view (achieves the best clustering performance).

Multi-view clustering methods: Partition level multiview subspace clustering(PMSC) [37], multiview consensus graph clustering(MCGC) [23], multiview graph learning (MVGL) [22], graph-based multi-view clustering(GMC) [24], autoencoder in autoencoder networks(AE²-NET) [38], reciprocal multi-layer subspace learning(RMSL) [39], and One2Multi

graph autoencoder clustering framework(O2MAC).

All the experiments are conducted using the released code on an Ubuntu-18.04 OS with an NVIDIA RTX 3090 GPU, and we have optimized the hyperparameters in their algorithms. Some methods cannot perform on all types of data, we only test them on partial datasets.

d) Implementation Details: In our experiments, we set $\lambda_1 = 0.01$ and $\lambda_2 = 0.001$ for all datasets. For multi-view data without predefined graph, we use k -NN algorithm to construct initial graphs. For image data and text data, Euclidean metric and Cosine metric are used as the distance metric to construct neighbor tree, respectively. For each nodes, $k_M = 3$ nearest neighbors are selected to compose positive pairs. Note that, our model is not sensitive to the k of initial k -NN graphs in a larger range, we set $k_G = 10$ for all datasets. K-means [33]

TABLE V
CLUSTERING RESULTS OF VARIOUS METHODS ON SINGLE-VIEW DATA WITH MULTIPLY ATTRIBUTE GRAPHS.

Datasets	Methods	ACC	NMI	ARI	AMI	F1
DBLP	KM [33]	0.3864 \pm 0.0061	0.1153 \pm 0.0049	0.0671 \pm 0.0080	0.1145 \pm 0.0049	0.3195 \pm 0.0055
	GAE [34]	0.5558 \pm 0.0139	0.3072 \pm 0.0073	0.2577 \pm 0.0061	0.3112 \pm 0.0080	0.5418 \pm 0.0124
	DAEGA [35]	0.8733 \pm 0.0000	0.6742 \pm 0.0000	0.7014 \pm 0.0000	0.6803 \pm 0.0000	0.8617 \pm 0.0000
	SDCN [36]	0.6497 \pm 0.0039	0.2977 \pm 0.0018	0.3099 \pm 0.0033	0.2950 \pm 0.0041	0.6377 \pm 0.0029
	O2MAC [18]	0.9012\pm0.0048	0.7250\pm0.0116	0.7806\pm0.0088	0.7267\pm0.0109	0.8981\pm0.0050
	CMGEC	0.9103\pm0.0039	0.7237\pm0.0021	0.7859\pm0.0062	0.7234\pm0.0030	0.9042\pm0.0042
IMDB	KM [33]	0.3154 \pm 0.0034	0.0119 \pm 0.0048	0.0028 \pm 0.0021	0.0109 \pm 0.0049	0.1799 \pm 0.0106
	GAE [34]	0.4298 \pm 0.0134	0.0402 \pm 0.0031	0.0403 \pm 0.0019	0.0398 \pm 0.0023	0.4620 \pm 0.0141
	DAEGA [35]	0.3683 \pm 0.0013	0.0055 \pm 0.0004	0.0039 \pm 0.0001	0.0059 \pm 0.0003	0.3560 \pm 0.0009
	SDCN [36]	0.4047 \pm 0.0030	0.0099 \pm 0.0009	0.0109 \pm 0.0011	0.0101 \pm 0.0008	0.3535 \pm 0.0029
	O2MAC [18]	0.4586\pm0.0280	0.0607\pm0.0311	0.0732\pm0.0254	0.0593\pm0.0296	0.4676\pm0.0444
	CMGEC	0.4844\pm0.0123	0.0514\pm0.0091	0.0469\pm0.0077	0.0510\pm0.0080	0.5101\pm0.0201
ACM	KM [33]	0.6753 \pm 0.0113	0.3253 \pm 0.0047	0.3077 \pm 0.0106	0.3249 \pm 0.0047	0.6779 \pm 0.0116
	GAE [34]	0.6990 \pm 0.0161	0.4771 \pm 0.0083	0.4377 \pm 0.0070	0.4803 \pm 0.0090	0.7025 \pm 0.0156
	DAEGA [35]	0.8909 \pm 0.0000	0.6430 \pm 0.0000	0.7046 \pm 0.0000	0.6339 \pm 0.0000	0.8906 \pm 0.0000
	SDCN [36]	0.8631 \pm 0.0052	0.5783 \pm 0.0088	0.6387 \pm 0.0110	0.5787 \pm 0.0080	0.8619 \pm 0.0060
	O2MAC [18]	0.9039\pm0.0042	0.6909\pm0.0087	0.7410\pm0.0110	0.6935\pm0.0089	0.9061\pm0.0101
	CMGEC	0.9089\pm0.0073	0.6912\pm0.0036	0.7232\pm0.0106	0.6909\pm0.0057	0.9072\pm0.0059

TABLE VI
CLUSTERING RESULTS OF DIFFERENT METHODS ON MULTI-VIEW DATA WITH COMMON ATTRIBUTE GRAPH.

Datasets	Methods	ACC	NMI	ARI	AMI	F1
Cora	KM [33]	0.3311 \pm 0.0322	0.1302 \pm 0.0334	0.0597 \pm 0.0194	0.1267 \pm 0.0335	0.2504 \pm 0.0343
	GAE [34]	0.5301 \pm 0.0386	0.3971 \pm 0.0259	0.2933 \pm 0.0243	0.3875 \pm 0.0235	0.5019 \pm 0.0435
	DAEGA [35]	0.6969\pm0.0002	0.5341\pm0.0004	0.4690\pm0.0001	0.5318\pm0.0005	0.6839\pm0.0003
	SDCN [36]	0.6024 \pm 0.0043	0.5004\pm0.0030	0.3902 \pm 0.0029	0.4991\pm0.0035	0.6184 \pm 0.0044
	MCGC [23]	0.3043 \pm 0.0000	0.0038 \pm 0.0000	0.0131 \pm 0.0000	0.0040 \pm 0.0000	0.3030 \pm 0.0000
	MVGL [22]	0.2371 \pm 0.0000	0.0631 \pm 0.0000	0.0266 \pm 0.0000	0.0599 \pm 0.0000	0.2574 \pm 0.0000
	GMC [24]	0.3667 \pm 0.0000	0.1389 \pm 0.0000	0.0301 \pm 0.0000	0.1914 \pm 0.0000	0.3182 \pm 0.0000
	CMGEC	0.7068\pm0.0304	0.4851 \pm 0.0184	0.4172\pm0.0204	0.4806 \pm 0.0184	0.6967\pm0.0189
Citeseer	KM [33]	0.4755 \pm 0.0584	0.2338 \pm 0.0457	0.2002 \pm 0.0461	0.2321 \pm 0.0458	0.4497 \pm 0.0582
	GAE [34]	0.3802 \pm 0.0167	0.1746 \pm 0.0179	0.1613 \pm 0.0215	0.1825 \pm 0.0180	0.3633 \pm 0.0435
	DAEGA [35]	0.6595 \pm 0.0001	0.4168\pm0.0000	0.4152\pm0.0000	0.4159\pm0.0001	0.6289 \pm 0.0000
	SDCN [36]	0.6596\pm0.0031	0.3871\pm0.0032	0.4017 \pm 0.0043	0.3913\pm0.0041	0.6362\pm0.0024
	MCGC [23]	0.3204 \pm 0.0000	0.1037 \pm 0.0286	0.0000 \pm 0.0000	0.1109 \pm 0.0000	0.2973 \pm 0.0000
	MVGL [22]	0.2816 \pm 0.0000	0.0803 \pm 0.0000	0.0225 \pm 0.0000	0.0815 \pm 0.0000	0.3043 \pm 0.0000
	GMC [24]	-	-	-	-	-
Pubmed	CMGEC	0.6765\pm0.0512	0.3666 \pm 0.0361	0.4072\pm0.0361	0.3650 \pm 0.0361	0.6549\pm0.0522
	KM [33]	0.5989 \pm 0.0009	0.3114\pm0.0031	0.2814\pm0.0014	0.3003\pm0.0040	0.5895 \pm 0.0004
	GAE [34]	0.6324 \pm 0.0167	0.2497 \pm 0.0259	0.2460 \pm 0.0268	0.2547 \pm 0.0260	0.6275 \pm 0.0179
	DAEGA [35]	0.6712\pm0.0000	0.2663 \pm 0.0001	0.2782 \pm 0.0001	0.2621 \pm 0.0000	0.6597\pm0.0002
	SDCN [36]	0.6578 \pm 0.0042	0.2947 \pm 0.0054	0.2546 \pm 0.0039	0.2959 \pm 0.0051	0.6516 \pm 0.0078
	MCGC [23]	0.4890 \pm 0.0000	0.1251 \pm 0.0000	0.1465 \pm 0.0000	0.1210 \pm 0.0000	0.5060 \pm 0.0000
	MVGL [22]	0.4604 \pm 0.0000	0.0463 \pm 0.0000	0.0094 \pm 0.0000	0.0501 \pm 0.0000	0.5039 \pm 0.0000
	GMC [24]	0.4025 \pm 0.0000	0.0173 \pm 0.0000	0.0050 \pm 0.0000	0.0264 \pm 0.0000	0.5203 \pm 0.0000
	CMGEC	0.7055\pm0.0087	0.3428\pm0.0043	0.3345\pm0.0050	0.3427\pm0.0039	0.6966\pm0.0102

is utilized to obtain the final cluster assignments according to the learned common representation.

B. Comparison of Clustering Performance

a) *Numerical Results Comparison:* In this section, the ACC, NMI, AMI, ARI and F1 are employed to compare the performance of the CMGEC with other 11 algorithms. Table IV, V and VI give the mean and variance of all the evaluation indexes obtained by all approaches. In these tables,

the top value is highlighted in red font and the second best in blue. From Table IV, V and VI, the following observations can be made: (1) overall, CMGEC achieves very competitive and stable performance compared to almost all baselines. In many cases, the improvements are very significant. This means that the common representations learned by our proposed method are effective. Taking the datasets 3Sources and 100Leaves for example, the ACC improvements of CMGEC over other baselines are about 4.93 and 9.18 percent, respectively; (2)

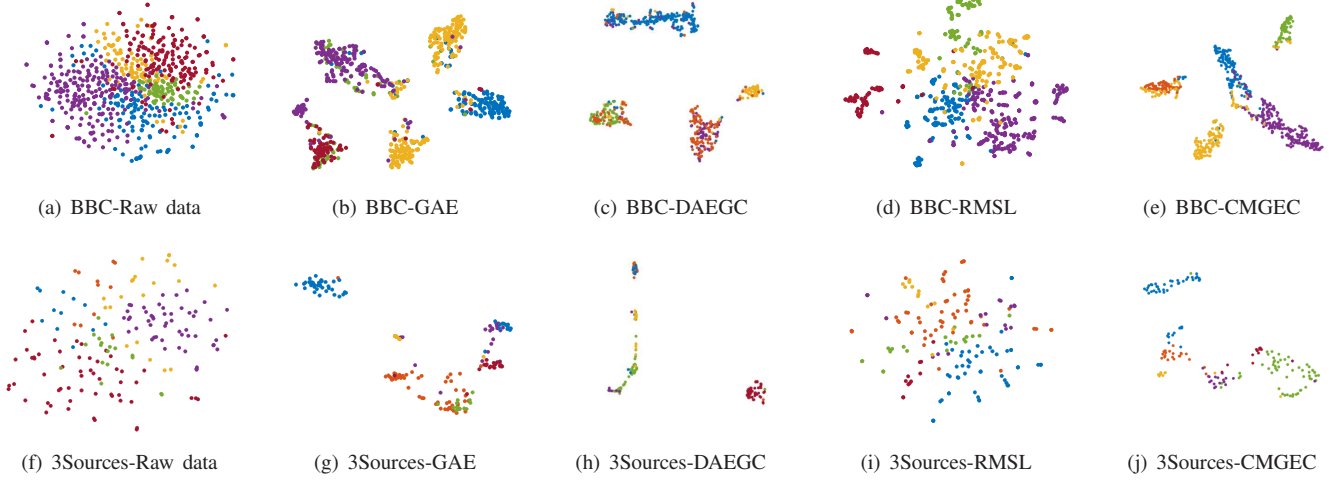


Fig. 3. t-SNE [43] visualizations of representations learned by various methods on BBC (top row) and 3Sources (bottom row).

although the performance of our method is not always top, the performance is rather robust across different datasets, while the performance of some methods is very unpredictable, even difficult to perform on some datasets. For example, for single-view data with multiply attribute graphs, O2MAC achieves comparable performance with our method. However, it is difficult to apply O2MAC directly to multi-view data. In addition, DAEGA achieves the promising performance on multi-view data with common attribute graph. However, on BBC and 100Leaves, it does not perform very well; (3) the performance of graph-based shallow methods is generally worse than GCN-based methods, confirming that it is useful to combine adjacent information with node characteristics; (4) the performance of many multi-view clustering methods is preferred to that of the single clustering methods with the best view result. For example, multi-view GCN-based method O2MAC and our CMGEC show superior performance with single-view GCN-based methods. This proves that it is effective to incorporate multiple views.

b) *Visualization of the clustering results:* In order to show the superiority of the representation obtained by our method, t-SNE [43] is used to visualize the embedded feature space of different methods. And the visualizations on BBC and 3sources are given in Fig. 3. From left to right, they are the space of raw data(best view), the results of GAE(best view), DAEGC(best view), RMSL, and our CMGEC, respectively. From Fig. 3, we can see that the representations obtained by our model are superior than that obtained by other algorithms which have clearer distribution structure.

C. Parameter sensitivity analysis

a) *The parameter sensitivity of k_G in predefined graph:* The number of the nearest neighbors k_G is an important parameter in the construction of the k -NN graph for data without predefined graph and has a great impact on the performance of most graph-based algorithms. To examine the effect of k_G , we design a k_G -sensitivity experiment on the BBC and 100Leaves datasets. It can be seen from Fig. 4 that our model is insensitive with $k_G \in \{5, 20\}$ compared

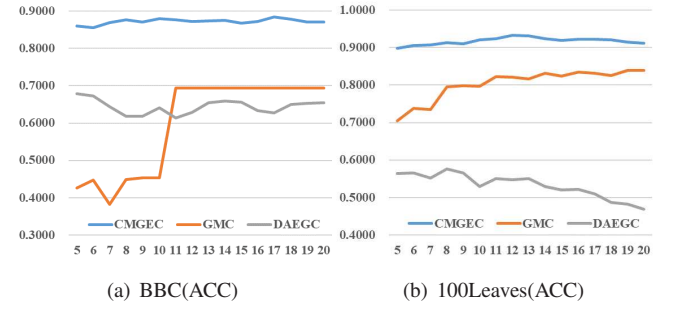


Fig. 4. The parameter sensitivity of k_G on BBC and 100Leaves datasets.

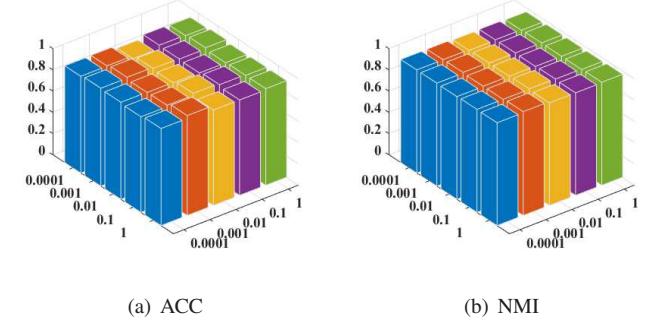


Fig. 5. The parameter effects of λ_1 and λ_2 on the BBC dataset with ACC and NMI metrics.

with GMC and DAEGC. It proves that our method can learn multi-view structural information even there are less neighbor information or some spurious connections. However, larger k_G can lead to more edges in the graph, which slows down the speed of the graph convolution. Thus, we set k_G to 10 for all datasets in our experiments.

b) *The parameter effect of λ_1 and λ_2 :* In our CMGEC model, there are two hyperparameters λ_1 and λ_2 that need to be set properly. In our experiments, we tune λ_1 and λ_2 from $\{0.0001, 0.001, 0.01, 0.1, 1\}$ and $\{0.0001, 0.001, 0.01, 0.1, 1\}$, respectively. Fig. 5 shows the results of our method using different parameters (taking BBC as an example). Here, we

TABLE VII
PERFORMANCE OF CMGEC AND ITS VARIANTS ON DIFFERENT DATASETS.

Datasets	Methods	ACC	NMI	ARI
3Sources	CMGEC	0.7653	0.6694	0.6049
	CMGEC-m	0.7459	0.6567	0.6027
	CMGEC-g	0.6568	0.6356	0.5967
	CMGEC-mg	0.6499	0.6360	0.5723
Cub	CMGEC	0.8467	0.7951	0.7117
	CMGEC-m	0.8395	0.7860	0.6994
	CMGEC-g	0.7767	0.7740	0.6601
	CMGEC-mg	0.7699	0.7749	0.6487
IMDB	CMGEC	0.4844	0.0514	0.0469
	CMGEC-m	0.4839	0.0520	0.0481
	CMGEC-g	0.4441	0.0414	0.0369
	CMGEC-mg	0.4395	0.0384	0.0376

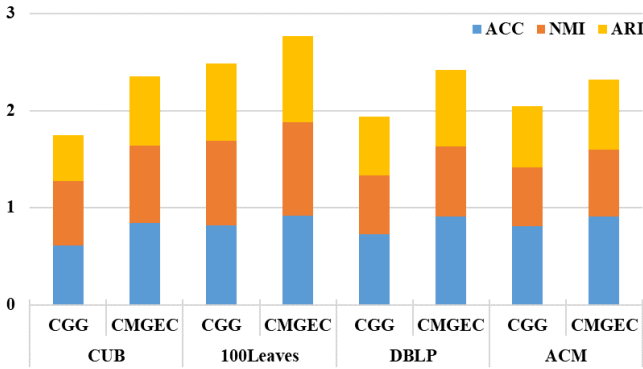


Fig. 6. Performance comparisons of CGG and CMGEC.

vary a parameter at a time while keeping another fixed. From Fig. 5, it can be seen that our method performs stably over a wide range of hyperparameter values.

D. Model Structure Analysis

a) *Clustering with consensus graph:* It is obvious that the clustering results can be obtained directly from the consensus graph A^* obtained by GFN. In order to show the superiority of the graph embedding, we conduct experiments on two datasets. The clustering results are given in Fig. 5, where CGG denotes the clustering results obtained by consensus graph segmentation. Apparently, CMGEC outperforms CGG in all datasets. This indicates that graph embedding can help to learn a suitable representation for clustering compared to consensus graph segmentation clustering.

b) *Performance Comparison of without MIM and GFN:* In order to show the effectiveness of the proposed MMIM and GFN, we conduct a series of experiments on three datasets. With other modules fixed, we change these two modules and analyze the following three approaches: (1) training the model without the MMIM(CMGEC-m); (2) training the model without GFN(CMGEC-g). The graph of the most informative view is used as the consensus graph; (3) training the model without the above two modules(CMGEC-mg). The clustering results are shown in Table VII. It can be seen that each

variants of our method has relatively high ACC, NMI, and ARI, and the best performance can be achieved on almost all datasets when using whole CMGEC. This indicates that GFN can learn a consensus graph that is more suitable for clustering compared with the graph of the most informative view. Moreover, optimizing similar samples of each view by MMIM is effective for clustering. It demonstrates that both GFN and MMIM are effective and cluster-friendly.

V. CONCLUSION

In this paper, we propose a Consistent Multiple Graph Embedding Clustering framework(CMGEC), which is mainly composed of Multiple Graph Auto-Encoder(M-GAE), Multi-view Mutual Information Maximization module(MMIM) and Graph Fusion Network(GFN). Specifically, M-GAE is devised to learn a common representation using a multi-graph attention fusion encoder and reconstruct multi-view graphs by view-specific decoders. By introducing a multi-graph attention fusion layer, the common representation can adaptively integrate complementary information from multiple views. In order to maintain the similarity of the neighboring characteristic, MMIM is introduced to make similar instances still similar to each other in the common space. Moreover, we design a GFN to explore complex relationships among different views and learn a consensus graph needed in M-GAE. And the rank constraint on its Laplacian matrix is further utilized to train the GFN to improve the separability of the consensus graph. By jointly training these models, a view consistent representation can be learned for clustering. Experiments on three types of multi-view datasets verify the advantage of our proposed method compared with state-of-the-art methods.

REFERENCES

- [1] A. Oliva and A. Torralba, “Modeling the shape of the scene: A holistic representation of the spatial envelope,” *Int. J. Comput. Vis.*, vol. 42, no. 3, pp. 145–175, 2001.
- [2] R. Manthalkar, P. K. Biswas, and B. N. Chatterji, “Rotation and scale invariant texture features using discrete wavelet packet transform,” *Pattern Recognit. Lett.*, vol. 24, no. 14, pp. 2455–2462, 2003.
- [3] C. K. Heng, S. Yokomitsu, Y. Matsumoto, and H. Tamura, “Shrink boost for selecting multi-lbp histogram features in object detection,” in *IEEE Conf. Comput. Vis. Pattern Recog.*, 2012, pp. 3250–3257.
- [4] N. Dalal and B. Triggs, “Histograms of oriented gradients for human detection,” in *IEEE Conf. Comput. Vis. Pattern Recog.*, 2005, pp. 886–893.
- [5] X. Gao, T. Mu, J. Y. Goulermas, and M. Wang, “Topic driven multi-modal similarity learning with multi-view voted convolutional features,” *Pattern Recognition*, vol. 75, pp. 223–234, 2018.
- [6] Y. Chen, X. Xiao, and Y. Zhou, “Jointly learning kernel representation tensor and affinity matrix for multi-view clustering,” *IEEE Transactions on Multimedia*, vol. 22, no. 8, pp. 1985–1997, 2020.
- [7] M. Yin, J. Gao, S. Xie, and Y. Guo, “Multiview subspace clustering via tensorial t-product representation,” *IEEE Trans. Neural Networks Learn. Syst.*, vol. 30, no. 3, pp. 851–864, 2019.
- [8] Y. Wang, X. Lin, L. Wu, W. Zhang, Q. Zhang, and X. Huang, “Robust subspace clustering for multi-view data by exploiting correlation consensus,” *IEEE Trans. Image Process.*, vol. 24, no. 11, pp. 3939–3949, 2015.
- [9] Y. Zheng, “Methodologies for cross-domain data fusion: An overview,” *IEEE Trans. Big Data*, vol. 1, no. 1, pp. 16–34, 2015.
- [10] Z. Kang, G. Shi, S. Huang, W. Chen, X. Pu, J. T. Zhou, and Z. Xu, “Multi-graph fusion for multi-view spectral clustering,” *Knowl. Based Syst.*, vol. 189, 2020.
- [11] K. Zhan, C. Niu, C. Chen, F. Nie, C. Zhang, and Y. Yang, “Graph structure fusion for multiview clustering,” *IEEE Trans. Knowl. Data Eng.*, vol. 31, no. 10, pp. 1984–1993, 2019.

[12] J. Wen, K. Yan, Z. Zhang, Y. Xu, J. Wang, L. Fei, and B. Zhang, “Adaptive graph completion based incomplete multi-view clustering,” *IEEE Transactions on Multimedia*, pp. 1–1, 2020.

[13] T. N. Kipf and M. Welling, “Semi-supervised classification with graph convolutional networks,” in *Int. Conf. Learn. Represent.*, 2017.

[14] M. S. Schlichtkrull, T. N. Kipf, P. Bloem, R. van den Berg, I. Titov, and M. Welling, “Modeling relational data with graph convolutional networks,” in *ESWC*, vol. 10843, 2020, pp. 593–607.

[15] C. Wang, S. Pan, R. Hu, G. Long, J. Jiang, and C. Zhang, “Attributed graph clustering: A deep attentional embedding approach,” in *IJCAI*, 2019, pp. 3670–3676.

[16] Z. Wang, L. Zheng, Y. Li, and S. Wang, “Linkage based face clustering via graph convolution network,” in *IEEE Conf. Comput. Vis. Pattern Recog.*, 2019, pp. 1117–1125.

[17] Z. Tao, H. Liu, J. Li, Z. Wang, and Y. Fu, “Adversarial graph embedding for ensemble clustering,” in *IJCAI*, 2019, pp. 3562–3568.

[18] S. Fan, X. Wang, C. Shi, E. Lu, K. Lin, and B. Wang, “One2multi graph autoencoder for multi-view graph clustering,” in *WWW*, 2020, pp. 3070–3076.

[19] S. Yun, M. Jeong, R. Kim, J. Kang, and H. J. Kim, “Graph transformer networks,” in *Adv. Neural Inform. Process. Syst.*, 2019, pp. 11960–11970.

[20] N. F. Chikhi, “Multi-view clustering via spectral partitioning and local refinement,” *Inf. Process. Manag.*, vol. 52, no. 4, pp. 618–627, 2016.

[21] J. W. Son, J. Jeon, A. Lee, and S. Kim, “Spectral clustering with brainstorming process for multi-view data,” in *AAAI*, 2017, pp. 2548–2554.

[22] K. Zhan, C. Zhang, J. Guan, and J. Wang, “Graph learning for multiview clustering,” *IEEE Trans. Cybern.*, vol. 48, no. 10, pp. 2887–2895, 2018.

[23] K. Zhan, F. Nie, J. Wang, and Y. Yang, “Multiview consensus graph clustering,” *IEEE Trans. Image Process.*, vol. 28, no. 3, pp. 1261–1270, 2019.

[24] H. Wang, Y. Yang, and B. Liu, “GMC: graph-based multi-view clustering,” *IEEE Trans. Knowl. Data Eng.*, vol. 32, no. 6, pp. 1116–1129, 2020.

[25] M. I. Belghazi, A. Baratin, S. Rajeswar, S. Ozair, Y. Bengio, R. D. Hjelm, and A. C. Courville, “Mutual information neural estimation,” in *Proceedings of the 35th International Conference on Machine Learning, ICML 2018, Stockholm, Sweden, July 10-15, 2018*, ser. Proceedings of Machine Learning Research, vol. 80, 2018, pp. 530–539.

[26] R. Gomes, A. Krause, and P. Perona, “Discriminative clustering by regularized information maximization,” in *Proceedings of Advances in Neural Information Processing Systems*, 2010, pp. 775–783.

[27] R. D. Hjelm, A. Fedorov, S. Lavoie-Marchildon, K. Grewal, P. Bachman, A. Trischler, and Y. Bengio, “Learning deep representations by mutual information estimation and maximization,” in *7th International Conference on Learning Representations, ICLR 2019, New Orleans, LA, USA, May 6-9, 2019*. OpenReview.net, 2019.

[28] P. Velickovic, G. Cucurull, A. Casanova, A. Romero, P. Liò, and Y. Bengio, “Graph attention networks,” *CoRR*, vol. abs/1710.10903, 2017.

[29] C. Li and S. Lin, “Social flocks: Simulating crowds to discover the connection between spatial-temporal movements of people and social structure,” *IEEE Trans. Comput. Soc. Syst.*, vol. 5, no. 1, pp. 33–45, 2018.

[30] J. Wen, N. Han, X. Fang, L. Fei, K. Yan, and S. Zhan, “Low-rank preserving projection via graph regularized reconstruction,” *IEEE Trans. Cybern.*, vol. 49, no. 4, pp. 1279–1291, 2019.

[31] W. Jiang, W. Liu, and F. Chung, “Knowledge transfer for spectral clustering,” *Pattern Recognit.*, vol. 81, pp. 484–496, 2018.

[32] R. A. Jarvis and E. A. Patrick, “Clustering using a similarity measure based on shared near neighbors,” *IEEE Trans. comput.*, vol. 100, no. 11, pp. 1025–1034, 1973.

[33] D. Sculley, “Web-scale k-means clustering,” in *WWW*, M. Rappa, P. Jones, J. Freire, and S. Chakrabarti, Eds., 2010, pp. 1177–1178.

[34] T. N. Kipf and M. Welling, “Variational graph auto-encoders,” *CoRR*, vol. abs/1611.07308, 2016.

[35] C. Wang, S. Pan, R. Hu, G. Long, J. Jiang, and C. Zhang, “Attributed graph clustering: A deep attentional embedding approach,” in *IJCAI*, 2019, pp. 3670–3676.

[36] D. Bo, X. Wang, C. Shi, M. Zhu, E. Lu, and P. Cui, “Structural deep clustering network,” in *WWW*, 2020, pp. 1400–1410.

[37] Z. Kang, X. Zhao, C. Peng, H. Zhu, J. T. Zhou, X. Peng, W. Chen, and Z. Xu, “Partition level multiview subspace clustering,” *Neural Networks*, vol. 122, pp. 279–288, 2020.

[38] C. Zhang, Y. Liu, and H. Fu, “Ae2-nets: Autoencoder in autoencoder networks,” in *IEEE Conf. Comput. Vis. Pattern Recog.*, 2019, pp. 2577–2585.

[39] R. Li, C. Zhang, H. Fu, X. Peng, J. T. Zhou, and Q. Hu, “Reciprocal multi-layer subspace learning for multi-view clustering,” in *Int. Conf. Comput. Vis.*, 2019, pp. 8171–8179.

[40] P. Welinder, S. Branson, T. Mita, C. Wah, F. Schroff, S. Belongie, and P. Perona, “Caltech-UCSD Birds 200,” California Institute of Technology, Tech. Rep. CNS-TR-2010-001, 2010.

[41] C. Szegedy, W. Liu, Y. Jia, P. Sermanet, S. E. Reed, D. Anguelov, D. Erhan, V. Vanhoucke, and A. Rabinovich, “Going deeper with convolutions,” in *IEEE Conf. Comput. Vis. Pattern Recog.*, 2015, pp. 1–9.

[42] Q. V. Le and T. Mikolov, “Distributed representations of sentences and documents,” in *International Conference on Machine Learning*, vol. 32, 2014, pp. 1188–1196.

[43] L. V. D. Maaten and G. Hinton, “Visualizing data using t-sne,” *Journal of Machine Learning Research*, vol. 9, no. 2605, pp. 2579–2605, 2008.